

Z. Shi  
Y. Li  
R. C. Wang  
Franz Makeschine

## Assessment of temporal and spatial variability of soil salinity in a coastal saline field

Received: 30 September 2004  
Accepted: 7 March 2005  
Published online: 21 May 2005  
© Springer-Verlag 2005

**Abstract** Many coastal tideland areas in southern Hangzhou Gulf in Zhejiang Province of China have been successively enclosed and reclaimed for agricultural land uses under a series of reclamation projects over the past 30 years. The variability of soil salinity was considerably great and an understanding of the temporal and spatial components of soil salinity variability is essential before decisions can be made about the feasibility of site-specific management. In this paper, a 5.35-ha field reclaimed in 1996 was selected as the study site and 112 bulk electrical conductivity ( $EC_b$ ) measurements were performed in situ by a hand held device in the topsoil (0–20 cm) at regular 20-m intervals across the field over a two-year period. Conventional statistics and geostatistical techniques were used to assess the spatial variability and temporal stability of soil-salinity distribution. The results indicated high coefficients of variation in topsoil salinity over the three samplings. Simple mean  $EC_b$  comparison revealed that soil salinity increased

from winter to spring. Kriged contour maps showed the spatial trend of salinity distribution and revealed the consistently high and low salinity areas of the field. In percentage terms, the proportions of the moderately saline class, strongly saline class, and extremely saline class were 37, 39, and 24%, respectively. Temporal stability map indicated that more than 60% of the study field was determined as the stable class. Based on the spatial and temporal characteristics, a similarity assessment map was created, which presented 5 homogenous sub-zones, each with different characteristics that can have an impact on the way the field is managed. It was concluded that saline soil land might be managed in a site-specific way based on the clearly defined management sub-regions within the field.

**Keywords** Soil salinity · Spatial variability · Temporal stability · Similarity assessment · Management sub-zone · Coastal saline soil · China

Z. Shi (✉) · Y. Li · R. C. Wang  
F. Makeschine  
Institute of Agricultural Remote Sensing  
and Information Technology Application,  
Department of Resource Science, College  
of Resource and Environmental Sciences,  
Zhejiang University, Hangzhou, 310029,  
China  
E-mail: shizhon@zju.edu.cn  
Tel.: +86-571-86971831  
Fax: +86-571-86971272

### Introduction

Rapid industrialization and urbanization have resulted in the loss of a significant amount of agricultural land since the economic reforms and an open-door policy in China. This is especially true in many southeast coastal regions and cities where maximizing economic efficiency

is the top priority of development. To alleviate the severe conflict between the ever-increasing population and the limited agricultural land resources, there is an urgent need for the reclamation of coastal tidelands. For example, in Zhejiang Province, a total of 400,000 ha tidelands have been reclaimed for agricultural land use and urbanization buffer zones under a series of

reclamation programs during the past 30 years. In Shangyu city of Zhejiang Province, approximately 17,000 ha coastal saline lands have been reclaimed, producing plenty of cottons, fruits, and aquatic products for the city (Shi et al. 2002a).

Owing to the differences in reclamation measures and farming practices, soil physical and chemical properties, especially soil salinity level in coastal tidelands, presented considerably large variability, which causes uneven crop growth, influences land-use planning according to soil suitability, confounds treatment effects in field experiments, and decreases the effectiveness of uniformly applied fertilizer on a field scale (Perrier and Wilding 1986; Miller et al. 1988; Mulla et al. 1990; Kang and Moorman 1997). Its consequences to the environment and to the production capacity have been the subject of research in the past for a range of climatic and edaphic conditions (Paz-González et al. 2000). Understanding and quantifying the magnitude, extent, and pattern of soil-salinity variability in space and time are necessary to define cost-effective management zones to manage variability in a site-specific way and to lead to better land-use patterns and high crop productivity (Doerge 1999; Huggins and Alderfer 1995). Previously, changes in soil properties were monitored through long-term field experiments and ecological research programs (Johnston et al. 1986). However, the implementation of such strategies is time consuming and often limited by cost, which is dominated by the expenses incurred in sampling and analysis. As an effective tool, a geostatistical method has been widely used to interpret spatial data, model spatial continuity and variability of soil properties in terms of the rate of change of regionalized variable and resolve site-specific problems (Miller et al. 1988; Chien et al. 1997). It has been viewed as one of the most precise estimators for spatial data analysis (Kitanidis 1997).

Although spatial and temporal variability of soil properties have been widely studied (Chevallier et al. 2000; Shi et al. 2002b; Mahmut and Cevat 2003; Sun et al. 2003), very few were reported on coastal saline soils that have been reclaimed for a few years. The objectives of this paper were to (1) characterize spatial distribution and variability of soil salinity in a coastal saline field; (2) analyze the temporal stability of soil

salinity and develop the temporal stability map; and (3) produce a similarity assessment map based on temporal-spatial variability and assess the likely potential for site-specific management of soil salinity in a coastal field.

## Materials and methods

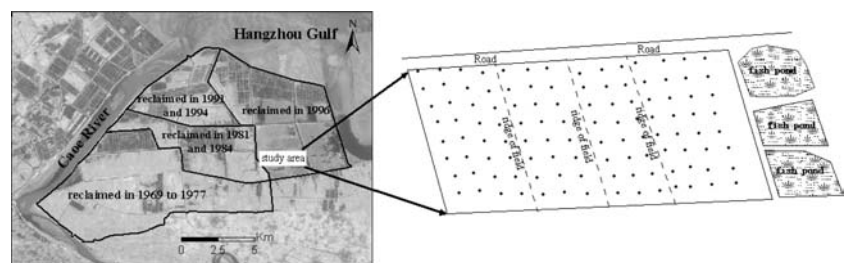
### Study site

The study area is in the northern region of Shangyu city, Zhejiang Province, at the south shore of Hangzhou Gulf, covering an area of 26,061 hectares ( $30^{\circ}04'00''$ – $30^{\circ}13'47''$  N,  $120^{\circ}38'32''$ – $120^{\circ}51'53''$  E). It belongs to the subtropical region with evergreen broad-leaved vegetation, an average annual temperature of  $16.5^{\circ}\text{C}$ , and an average annual precipitation of 1,300 mm. The dominant soils were formed by modern marine and fluvial deposit matters. Soil textures are light loam or sandy loam, with a high concentration of Na- and Mg-salts ( $>1\%$ ). Over the past 30 years, many coastal tideland areas have been successively reclaimed for agricultural land uses. The study was conducted in a 5.35-ha field, which was reclaimed in 1996 (Fig. 1).

### Data collection

A regular grid-sampling scheme (20-m sampling space) was imposed on the field to select points of measurements. Bulk electrical conductivity ( $\text{EC}_b$ ) measurements for topsoil (0–20 cm) were performed on each grid point in situ using a portable WET sensor and 112 composite  $\text{EC}_b$  readings were obtained. The three sampling dates were November 7, 2003, January 2, 2004, and April 29, 2004, respectively. Each  $\text{EC}_b$  measurement was georeferenced using a trimble GPS (with differential correction). The GPS receiver accuracy was within 2 m of horizontal accuracy. At each regular spacing point, 5 samplings within a 1-m circle were measured by inserting the sensor probes into the soil and then the average reading was computed as the  $\text{EC}_b$  value at that point. Meanwhile, some soil samples were collected and taken

**Fig. 1** Location of the study area in Shangyu city and spatial distribution pattern of samples



back to the laboratory. EC1:5 readings were measured by a conventional conductivity meter in a 1:5 (soil/water) suspension and then compared with those from WET sensor.

Figure 2 reveals that EC1:5 readings were linearly well correlated with  $EC_b$  readings for the three samplings. In other words, the  $EC_b$  readings can be used to replace EC1:5 readings to a great extent with an acceptable accuracy, especially in a considerably large area. The general regression equation can be expressed by the following formula:  $y = 0.798x + 18.3$ , where  $y$  denotes the EC1:5 readings and  $x$  denotes the  $EC_b$  readings. Thus, EC1:5 readings can be easily obtained by utilizing the  $EC_b$  data from the field method, which has its advantages with an acceptable cost. For example, the price of the wet sensor was only 3,500 dollars, whereas one sample analyzed in the lab cost 2.5 dollars. So, to evaluate the temporal and spatial variability, which need frequent sampling and analysis, the field method is more economic and time-saving than the sample collection.

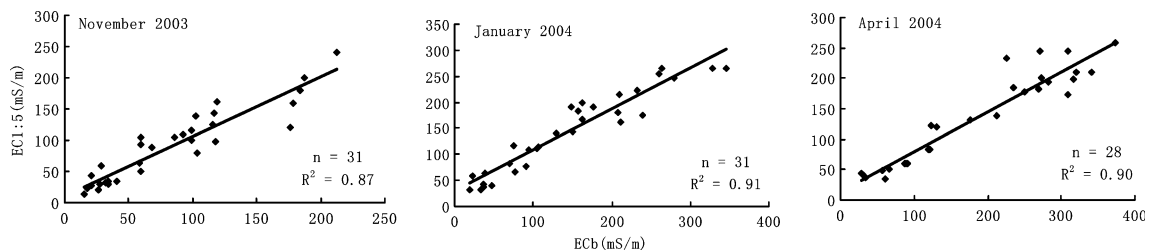
### Geo-statistics and spatial interpolation

Semi-variogram analyses were carried out on all the datasets. Isotropic spherical models were used to fit the experimental semi-variograms. Ordinary kriging was chosen to estimate the values at the unknown positions. Smoothed contour maps of soil  $EC_b$  on the three different sampling dates, of mean  $EC_b$  at each sampling point and of the associated coefficients  $CV_i$  over the two-year period (see section below), were then produced using the interpolated values.

Each dataset was interpolated into a regular 10-m grid to enable calculations to be implemented in a spreadsheet using the data from coincident grid points, and 34 rows and 18 columns were given. After blanking the grids outside the field boundary, 535 points remained.

All the geostatistical computations were performed by using the GS + 3.1 version for windows and ArcGIS 8.3 software package.

**Fig. 2** Correlation coefficient ( $R^2$ ) between the EC1:5 readings and  $EC_b$  readings on the three sampling dates



### Temporal stability analysis

The temporal stability was assessed by calculating the coefficient of variation over time at each sampling point to estimate the stability of  $EC_b$ . The technique has been used by Blackmore (2000) to assess the temporal stability of crop yields and by Shi et al. (2002a) to assess the soil properties in grasslands.

$$CV_i = \frac{\sqrt{\frac{\left( n \times \sum_{t=1}^n EC_{b_{it}}^2 - \left( \sum_{t=1}^n EC_{b_{it}} \right)^2 \right)}{(n \times (n-1))}}{\sum_{t=1}^n EC_{b_{it}} / n}, \quad (1)$$

where  $CV_i$  is the coefficient of variation over time at the  $i$ th sampling point;  $EC$  is the measured value of soil  $EC_b$  at the  $i$ th sampling point in the  $t$ th time;  $n$  is the number of field samplings.

### Similarity assessment of salinity variability pattern

The maps that quantify the spatial and temporal variability of soil  $EC_b$  can be further combined into a single map, a similarity assessment map, to represent areas of the field according to their spatial and temporal characteristics, which can be used by managers for further decision-making and management purposes.

The empirical formula between EC1:5 and total salt content was founded in this study site by Wu and Chen (1981). Due to the high correlation of  $EC_b$  with EC1:5 (Fig. 2),  $EC_b$  was transformed into total salt content using this empirical formula. According to the classification for saline soil by Bao (2000), three categories were classified: moderately saline ( $66-136 \text{ mS.m}^{-1}$ ), strongly saline ( $136-204 \text{ mS.m}^{-1}$ ), and extremely saline ( $> 204 \text{ mS.m}^{-1}$ ).

By comparing the  $CV_i$  to an arbitrary threshold, the temporal stability of  $EC_b$  for coastal saline soil was classified into two classes: stable ( $CV_i < 20\%$ ) and unstable ( $CV_i \geq 20\%$ ).

Table 1 lists the assessment classes and their conditions. Each class was derived from the two previous datasets by applying combinational logic statements. Condition 1 identified which category the point belonged to; condition 2 identified the stability of the

**Table 1** Similarity assessment classes and their conditions

Assessment classes	Condition 1		Condition 2
	EC <sub>b</sub> content (mS.m <sup>-1</sup> )	Total salt content (%)	CV <sub>i</sub> (%)
Moderately saline and stable (MSS)	66–136	0.2–0.4	< 20
Moderately saline and unstable (MSU)	66–136	0.2–0.4	≥20
Strongly saline and stable (SSS)	136–204	0.4–0.6	< 20
Strongly saline and unstable (SSU)	136–204	0.4–0.6	≥20
Extremely saline and stable (ESS)	> 204	> 0.6	< 20

salinity at the point. If both conditions were true, then a point was considered to belong to a particular class. In the present study, there were 5 classes: Moderately saline and stable (MSS), Moderately saline and unstable (MSU), Strongly saline and stable (SSS), Strongly saline and unstable (SSU), and Extremely saline and stable (ESS).

## Results

### Data exploration and classical statistical analyses

Before more formal geostatistical analysis, the data were first explored to remove some abnormal values and classical statistical analysis was then performed. To overcome the difficulties arising from departures from normality, a log-normal transform was used to make the measured EC<sub>b</sub> values to be normal distribution. The descriptive statistics for original and transformed EC<sub>b</sub> at the three sampling dates are summarized in Table 2. As commonly reported, coefficients of variations (CVs) of salinity measurements were fairly high (Mahmut and Cevat 2003; Warrick and Nielsen 1980). This can be due to uneven crop growth, not uniform management practices, and the undulating topography, which resulted in a marked change in topsoil salinity even over small distances. The original EC<sub>b</sub> datasets indicated a right-skewed distribution showing asymmetry (skewness > 0), which can be attributed to the mechanism of successive random dilutions (Ott 1995) and to the high variability observed in the study.

**Table 2** Descriptive statistics of original EC<sub>b</sub> (mS.m<sup>-1</sup>) and transformed EC<sub>b</sub> at the three sampling dates

Sampling date	Mean	SD	CV(%)	Range	Skewness	Kurtosis
Nov 2003						
Original EC <sub>b</sub>	139.4	64.9	47	50.2–310.5	0.64	2.51
Log EC <sub>b</sub>	4.83	0.5	9.7	3.9–5.7	0.02	1.81
Jan 2004						
Original EC <sub>b</sub>	159.7	75.1	47	52.8–329.7	0.42	2.05
Log EC <sub>b</sub>	4.96	0.51	10.1	4.0–5.8	-0.11	1.68
Apr 2004						
Original EC <sub>b</sub>	176.8	67.0	38	70–301	0.21	1.84
Log EC <sub>b</sub>	5.10	0.4	7.8	4.3–5.7	-0.22	1.78

As shown in Table 2, the means and standard deviations of the EC<sub>b</sub> varied over the three samplings. The mean EC<sub>b</sub> of the study site increased from 139.4 mS.m<sup>-1</sup> to 176.8 mS.m<sup>-1</sup> and the salinity level in April 2004 was the highest, which can be influenced by upward transport of salts in groundwater with evaporation. According to the reports by Fu et al. (2001), the salinity of surface layers of the soil profile increases when the saline groundwater table is very close to the soil surface during the spring rain months. The low salinity content in November 2003 was due to less transpiration under moderate temperatures and continuously rainless weather. In addition, some fresh water irrigated into the field and diluted the salinity content in the topsoil.

### Semi-variance analyses and spatial trend analyses

Analysis of spatial dependence of soil salinity illustrated an isotropic behavior. Figure 3 plots the experimental semi-variances and the fitted semi-variogram models for the EC<sub>b</sub> at the three sampling dates, and the parameters for these models are given in Table 3. The semi-variograms expressed the spatial behavior of the regionalized variable EC<sub>b</sub>, and all of them had good continuity in space, and they can be modeled quite well with spherical models.

The semi-variance values of each of the three datasets displayed similar tendencies. As presented in Fig. 3, the range values and C<sub>0</sub>/C ratios did not change significantly between the three different samplings, which revealed that the spatial structure of the variability had remained

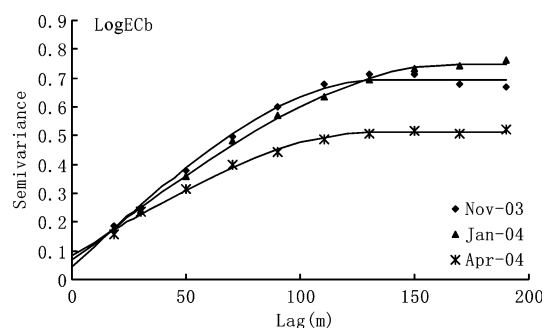


**Fig. 3** Semi-variances and their fitted model (solid line) for soil  $EC_b$  at three sampling dates

relatively stable with time. The presence of nugget variance for the three datasets implied the variability over distances shorter than the sampling space ( $< 20$  m) and other unaccountable measurement errors. The ratio of nugget effect to sill, expressed in percentages, can be regarded as a criterion to classify the spatial dependence of soil properties (Chien et al. 1997; Chang et al. 1998). From Table 3, it can be seen that the ratios of nugget variance to sill variance for  $EC_b$  at the three sampling dates were all less than 25%. This demonstrated that the soil  $EC_b$  had strong spatial dependence, which can usually be attributed to intrinsic factors such as soil parent material (with high concentration of Na- and Mg-salts).

The range of spatial dependence is considered as the distance beyond which the observations are not spatially dependent, ranging from 133.7 m to 169.1 m, which indicated that the grid spacing (20 m) was adequate for the characterization of the spatial variability of soil salinity at the three sampling dates. Hajrasuliha et al.

**Table 3** Model and parameters of semi-variogram for  $EC_b$  at the three sampling dates after log-normal transformation

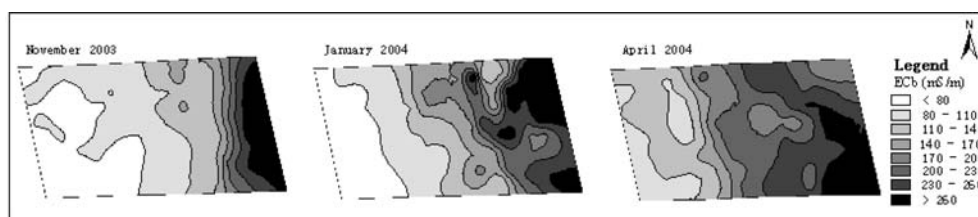
Sampling date	Fitted model	Nugget variance	Sill value	Nug/sill ratio (%)	Range (m)
November 2003	Spherical	0.046	0.695	6.6	135.6
January 2004	Spherical	0.068	0.75	9.1	169.1
April 2004	Spherical	0.082	0.512	16	133.7

(1980) reported that measurements of soil salinity on an 80-m grid were spatially dependent for a separation distance up to 800 m. Agrawal et al. (1995) also found that surface soil salinity measurements showed spatial dependence over a range of distances from 46 m to 119 m, depending on the grid size used in sampling. In a recent work by Utset et al. (1998), the range of influence of  $E_{ce}$  measurements on a 50-m grid was 500 m. However, the cases where no spatial structure was found for soil salinity were also reported, which were attributed to limited number of samples or size of sampling (Miyamoto and Cruz 1986). These findings and the author's work confirm that the sampling interval and inherited variability of salinity influence variance structure and range of spatial dependence.

Kriging interpolation was applied to  $EC_b$  data. This allowed the division of the plot into several classes to determine homogenous zones. The smoothed contour maps obtained for the three sampling dates are presented in Fig. 4.

From these maps, the spatial distribution of soil salinity can be easily recognized, which is helpful in management on fertility, analyzing experimental data to reduce subjective judgement, and developing and applying agronomic practices. The smoothed contour maps of each soil  $EC_b$  dataset displayed quite similar patterns with a high salinity level in the east corner and low salinity level in the west corner of the field, which illustrated that the salinity distribution for the three samplings had a similar trend and can be represented by the spatial trend map to show the consistently high and low salinity areas of the field. The high salinity level in the east edge was induced by the salinity in the groundwater. As there were some fish ponds east of the field, and plenty of groundwater can be filtered into the east edge of the study area, the upward transport of salts with evaporate resulted in the high salinity content. In addition, because of the coarse soil texture of sandy loam, salt leaching with rainfall and upward transport with evaporation were highly frequent, which resulted in the trait of quick salt leaching and accumulation in the topsoil in the coastal field. It has been reported that for the same coastal region, salts from the groundwater table which is below 3 m depth can be upward transported in the dry months and cause the accumulation of salinity in the topsoil (Ding et al. 2001). The low salinity content

**Fig. 4** Smoothed contour maps produced by ordinary kriging for bulk electrical conductivity at three different sampling dates



in the west edge reflected the influence of soil management practices.

The mean  $EC_b$  at each sampling point was calculated and a spatial trend map displayed three classes and the three class boundaries are defined according to the indices as listed in Table 1. There were 196 10-m grids (1.96 ha or 37%) in the moderately saline class, 209 (2.09 ha or 39%) in the strongly saline class, and 130 (1.3 ha or 24%) in the extremely saline class. The distribution is presented in Fig. 5.

Determining to what extent the investigated field is being affected by salinity and how it is spatially changing allows the farmers to understand what plant species can be grown successfully, and to determine the effectiveness of salinity management options. In fact, for the studied area, cotton was the main crop for its high salinity tolerance threshold. If some other crops with low salinity tolerance thresholds were to be planted, special management must be put into practice based on the previously defined sub-regions within the field, i.e. each mean  $EC_b$  class can be regarded as one sub-unit to manage salinity variability separately and to make decisions for appropriate crop plantation. According to Rhoades and Miyamoto (1990), salinity tolerance thresholds for corn and cotton plantations are 170 and 770  $mS.m^{-1}$ , respectively. Therefore, cotton can be planted in all the three sub-regions even in the extremely saline zone (204–298  $mS.m^{-1}$ ), whereas corn cannot be planted in this zone until the salinity level is reduced, but corn can be planted in the lands with lower salinity levels such as in the moderately saline zone (66–136  $mS.m^{-1}$ ). In addition, the area for each sub-region within the field was computed, which can be used to evaluate the economical feasibility of treatment and management in a site-specific manner.

**Fig. 5** Spatial trend map produced by ordinary kriging for mean  $EC_b$  (left figure) and number of grids in each mean  $EC_b$  class (right figure)

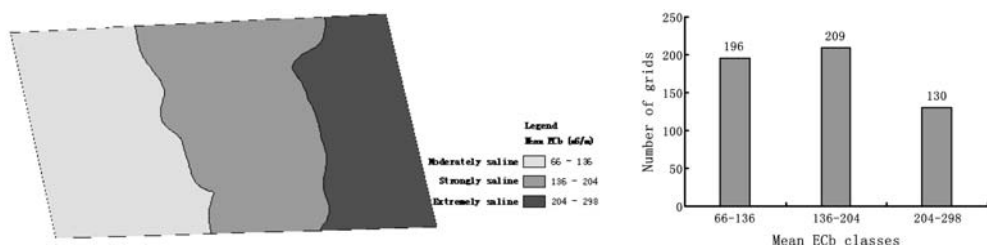
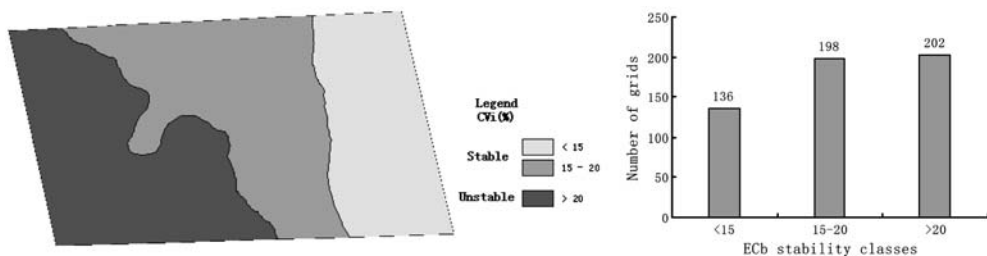


**Fig. 6** Temporal stability map produced for  $EC_b$  based on the  $CV_i$  assessment method (left figure) and number of grids in each  $EC_b$  stability class (right figure)



## Temporal stability analyses

The temporal stability map was produced by calculating the coefficients of variation over time ( $CV_i$ ) at each of the sampling points. The resulting map is presented in Fig. 6, which shows the stable areas that had not changed from year to year as well as the unstable areas that had been highly changeable. Three arbitrary classes were chosen at 5% intervals.

Of the 536 10-m grids in the dataset, there were 136 (1.36 ha or 25%) in the most stable class, 198 (1.98 ha or 37%) in the next class, and 202 (2.02 ha or 38%) in the unstable class. The distribution, seen in Fig. 6, was skewed towards the stable class in which the coefficient of variation was smaller than 20%.

Interestingly, it can be found that the east region with a high salinity content displayed temporal stability, whereas the west region with a lower salinity level showed temporal instability. Why these changes occurred is not readily apparent and still needs further investigation and analysis.

## Similarity assessment map

The similarity assessment map was a synopsis of the important features found in the spatial trend and temporal stability maps. The map has been heavily smoothed to show more accurate and practical management areas. It has five classes, with each threshold being taken from the relevant source map. The five classes are: Moderately saline and stable (MSS), Moderately saline and unstable (MSU), Strongly saline and stable (SSS), Strongly saline and unstable (SSU), and Extremely saline and stable (ESS).

The similarity assessment map presented the size and position of the spatial and temporal features. There were 27 10-m grids (0.27 ha or 5%) in the MSS class, 169 (1.69 ha or 32%) in the MSU class, 176 (1.76 ha or 33%) in the SSS class, 33 (0.33 ha or 6%) in the SSU class, and 130 (1.3 ha or 24%) in the ESS class, as shown in Fig. 7. It can be seen that 89% of the data are in the MSU (Moderately saline and unstable) class, SSS (Strongly saline and stable) class, and ESS (Extremely saline and stable) class.

According to the  $EC_b$  assessment classes, the studied field can be divided into five management sub-zones. This being the case, site-specific management of soil salinity can be conducted on the basis of soil measurements for each management sub-zones. Another purpose for creating the assessment map was to indicate homogenous areas for investigation or sampling. Spatial investigation is often implemented by sampling on regular grids, which can be expensive, whereas targeted sampling can be used for specific features for analysis. If investigation or sampling were carried out, the maxima and minima of large homogenous areas would be the first ones to be considered. In addition, the similarity assessment map gives the farmer an indication whether to focus on spatial or temporal management. If the spatial variability is seen to be significant, then the factors that result in the variability can be determined, treating the area differently is another. If temporal instability is seen to be significant, then frequent assessment of those areas may give some indication as to the cause. The faster it changes, the more often it must be assessed.

According to the ridges of the field (as shown in Fig. 1), the studied area can be divided into four fields: field I, field II, field III, and field IV. Different fields had different similarity, which illustrated the differences in farming practices. Field II displayed the most heterogeneous sub-zones, and investigation proved the presence of a small dyke, which resulted in the high heterogeneity in field II. The result suggested that a denser sampling strategy (< 20-m interval) should be taken in field II if more detailed variations in salinity content were to be known, and a nested sampling scheme would be rational in the whole study site to create kriged contour maps and to show accurately how the salinity varies with space and time.

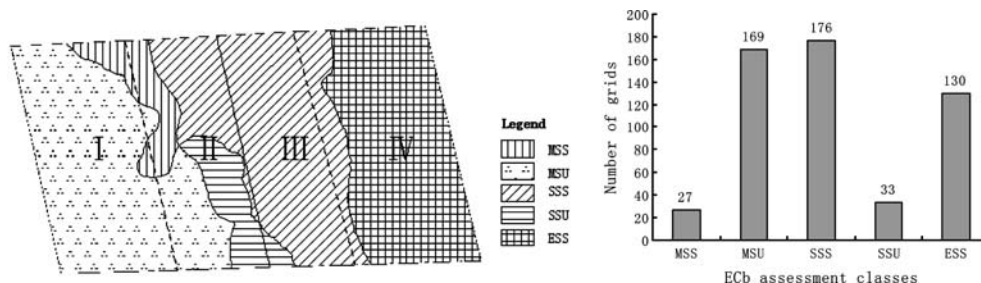
## Conclusions

To obtain more realistic intra-field zones for field management, a better knowledge of the spatial or temporal heterogeneities is necessary. In this paper, Geostatistical tools combined with other methods were used to identify spatial and temporal features of soil salinity in a coastal field and determine the homogenous sub-zones to implement special management for areas with similar variability. The analysis of the spatial distribution and trend maps revealed the relatively high salinity in the east edge, which can be explained by the presence of fish ponds along the field boundary. This conclusion is worth noting by the farmer to take measures to decrease the salinity content for high crop productivity and economic return. The temporal stability analysis of salinity data could help to know how the salinity changes with time and understand the influence of these changes on the crop in various conditions. The similarity assessment map can be used to manage soil salinity in a site-specific manner; although the small size of some zones does not justify separate treatment, attention should be paid to the similarity of variability.

Considering the results obtained on the experimental field, it appears that the delineation of homogenous zones not only can be useful to manage soil salinity in a site-specific manner, but can be used as an alternative to grid soil sampling to develop nutrient maps for variable rate fertilizer application. Zones that are not continuous (with high heterogeneity) should be sampled and managed separately, whereas the continuous zones can be sampled sparsely and managed uniformly. Indeed, the knowledge of such zones may serve to limit the amount of soil analysis to perform inside the field, and to precisely know where to take the samples to create application maps for the modulation of certain cultivation operations.

Further investigation would be needed on a range of coastal soil sites, however, before any conclusion could be reached regarding the general applicability of site-specific management in a coastal saline field.

**Fig. 7** Similarity assessment map of  $EC_b$  based on the spatial trend map and temporal stability map (left figure) and number of grids in each  $EC_b$  class (right figure)



## References

- Agrawal OP, Rao KVGK, Chauhan HS, Khandelwal MK (1995) Geostatistical analysis of soil salinity improvement with subsurface drainage system. *Trans ASAE* 38(5):1427–1433
- Bao SD (2000) Soil and agricultural chemistry analysis (In Chinese). Chinese Agriculture Press, Beijing, China, p 179
- Blackmore S (2000) The interpretation of trends from multiple yield maps. *Comput Electro Agr* 26:37–51
- Chang YH, Scrimshaw MD, Emmerson RHC, Lester JN (1998) Geostatistical analysis of sampling uncertainty at the Tollesbury Managed Retreat site in Blackwater Estuary, Essex, UK: kriging and cokriging approach to minimise sampling density. *Sci Total Environ* 221:43–57
- Chevallier T, Voltz M, Blanchart E, Chotte JL, Eschenbrenner V, Mahieu M, Albrecht A (2000) Spatial and temporal changes of soil C after establishment of a pasture on a long-term cultivated vertisol (Martinique). *Geoderma* 94:43–58
- Chien YJ, Lee DY, Guo HY, Hough KH (1997) Geostatistical analysis of soil properties of mid-west Taiwan soils. *Soil Sci* 162:291–297
- Ding NF, Li RA, Dong BR, Fu QL, Wang JH (2001) Orientation observation and study of salinity content and nutrient in newly reclaimed sandy soil. *Chinese J Soil Sci* 32(2):57–59 (in Chinese)
- Doerge T (1999) Defining management zones for precision farming. *Crop Insights* 8(21):1–5
- Fu QL, Li RA, Ge ZB (2001) Study on agricultural demonstration management zones in coastal region in Zhejiang province. In: Ding NF, Wang JH, Fu QL, Dong BR (eds) Study on water and salt movement of groundwater in coastal regions in north Zhejiang province (in Chinese). Zhejiang University Press, Hangzhou China, pp 74–77
- Hajrasuliha S, Baniabbassi N, Metthey J, Nielsen DR (1980) Spatial variability of soil sampling for salinity studies in southwest Iran. *Irrig Sci* 1:197–208
- Huggins DR, Alderfer AD (1995) Yield variability within a long-term corn management study: implications for precision farming. In: Robert PC, Rust RH, Larson WE (eds) Site-specific management for agricultural system. Proceedings of the 2nd International Conference. ASA, CSSA, and SSSA, Madison, WI, USA, pp 417–426
- Johnston AE, Goulding KWT, Powlton PR (1986) Soil acidification during more than 100 years under permanent grassland and woodland at Rothamsted. *Soil Use Manag* 2:3–10
- Kang BT, Moormann FR (1997) Effect of some biological factors on soil variability in tropics. Effect of precleaning vegetation. *Plant Soil* 47:441–449
- Kitanidis PK (1997) Introduction to geostatistics: application in hydrogeology. Cambridge University Press, Cambridge UK
- Mahmut C, Cevat K (2003) Spatial and temporal changes of soil salinity in a cotton field irrigated with low-quality water. *J Hydrol* 272:238–249
- Miller MP, Singer MJ, Nielsen DR (1988) Spatial variability of wheat yield and soil properties on complex hills. *Soil Sci Soc Am J* 52:1547–1553
- Miyamoto S, Cruz I (1986) Choosing functions for semi-variograms of soil properties and fitting them to sampling estimates. *J Soil Sci* 37:617–639
- Mulla DJ, Bhatti AU, Kunkel R (1990) Methods for removing spatial variability from field research trial. *Adv Soil Sci* 13:201–213
- Ott WR (1995) Environmental statistics and data analysis. Lewis Publishers, New York, p 313
- Paz-González P, Vieira SR, Taboada Castro MT (2000) The effect of cultivation on the spatial variability of selected properties of an umbric horizon. *Geoderma* 97:273–292
- Perrier ER, Wilding LP (1986) An evaluation of computational methods for field uniformity studies. *Adv Agron* 39: 265–312
- Rhoades JD, Miyamoto S (1990) Testing soils for salinity and sodicity Soil testing and plant analysis. In: Westerman RL (ed) Soil Science Society of American, Inc. Madison, Wisconsin USA, pp 299–366
- Shi Z, Wang K, Bailey JS, Jordan C, Higgins AH (2002a) Temporal changes in the spatial distribution of some soil properties on a temperate grassland site. *Soil Use Manag* 18:353–362
- Shi Z, Wang RC, Huang MX (2002b) Detection of coastal saline land uses with multi-temporal landsat images in Shangyu City, China. *Environ Manag* 30(1):42–150
- Sun B, Zhou SL, Zhao QG (2003) Evaluation of spatial and temporal changes of soil quality based on geostatistical analysis in the hill region of subtropic China. *Geoderma* 115:85–99
- Utset A, Ruiz ME, Herrera J, de Leon DP (1998) A geostatistical method for soil salinity sample site spacing. *Geoderma* 86:143–151
- Warrick AW, Nielsen DR (1980) Spatial variability of soil physical properties in the field. In: Hillel D (ed) Applications of soil physics. Academic Press, New York, pp 319–344
- Wu YW, Chen TQ (1981) Empirical formulae for the determination of total salt content by electric conductivity of coastal saline soils in Zhejiang province. *J Zhejiang Agric Univ* 7(2):125–128 (In Chinese)